Journal of Multidisciplinary Engineering Science Studies (JMESS)
ISSN: 2458-925X
Vol. 2 Issue 8, August - 2016

Improving The Electrical Properties Of Porous Silicon Photovoltaic Detector By Depositing CNTs

Ahmed J. Mhawes
Department of physiology, University of Kufa, Najaf, Iraq
Corresponding author, E-mail: ahmed_naji_abd@yahoo.com

***Abstract*— Now this article, porous silicon (PSi) photovoltaic detector prepared by electrochemical etching process at etching current density 14mA/cm^2 for 17min etching time, the suspension of multiwall carbon nanotubes deposited on the etched silicon (PSi) substrate. The characteristics of porous silicon and MWCNTs were investigated by using x-ray diffraction (XRD), atomic force microscopy (AFM), Fourier transformation infrared spectroscopy (FTIR), photoluminescence (PL), and scanning electron microscopy (SEM), current-voltage (I-V) characteristics, capacitance-voltage characteristics(C-V), spectral responsivity (Rλ) and specific detectivity of photodetectors were studied before and after depositing. Important improvement was seen in responsivity and specific detectivity of the porous silicon photovoltaic detector after depositing the MWCNTs into the matrix of porous.**

Keywords—porous silicon, electrical properties, photovoltaic detectors, I-V, C-V ,responsivity

Introduction : There is a rising demand of extremely efficient solid devices for a wide range of uses in various disciplines. Among the applicant materials, porous silicon (PSi) has drawn an increasing research attention, aside from its understandable potentially candid integration with the ordinary Si technologies, and this one existing applications span from biomedicine to biosensing, from Photonics to photovoltaic devices[1][2].

The visible light emitted from PSi, despite the crystalline Silicon band-gap of (1.12eV) at room temperature was assigned to the quantum size effects in the nanometer-sized Si crystallites. It was shown, as well, that luminescence wavelength can be tuned in a broad range and relatively high quantum efficiencies were achieved, improving the chance of using silicon for light emitting devices[3].CNTs are molecular-scale tubes of graphitic carbon with exceptional characteristics. They are among the hardest and most powerful fibers identified, which had significant electronic characteristics and many other un usual properties. CNTs are chemically steady, mechanically widely storing and conduct electricity. Because of these reasons the new perspectives for various applications was open up, like nanotransistors in circuits, field emission displays, artificial muscle or added supports in alloys. They exhibit unusual strength and unique electrical properties and are effective conductors of heat[4]. Their rising carrier mobility over their one dimension axes[5] [6] and ballistic transport properties, films of carbon nanotube had been considered as the best substitution for silicon in future optoelectronic equipment [7].

Experiment

In this study, single crystalline n-Si wafer of 4.5Ωcm electrical resistivity and orientations of (100) was used. The silicon wafer was etched by electrochemical etching (ionization) process, the silicon sample was etched at 14mA/cm^2 etching current density for etching time 17min at room temperature. The sample was clipping into (1.5 cm × 1.5 cm) square area. After (HF and ethanol) treating on the backside of the sample, 0.1μm thick high purity Al film by using thermal evaporation process was deposited.

Etching process was carried out by using a cell of Teflon with an electrolyte including 40% hydrofluoric acid(HF) mixed with 99.9% ethanol, by volume 1:2. 0.068mg/mL concentration MWCNTs powder with (10–60) nm diameter and length (10–15)μm supplied from Nano Tech Labs, Inc. USA were scattered in ethanol by aid of sonication for 8 hours as illustrated in Fig. 1. Drop casting process was used to deposit the MWCNTs on PSi substrate. Structural, morphological and optical properties of PSi and MWCNTs were examined by means of (CuKα) XRD-6000,Shimadzu x-ray diffractometer, Fourier transformation infrared spectroscopy, JEOL (JSM-5600) scanning electron microscopy and Angstrom AA 3000 atomic force microscopy . Structural, morphological, optical and electrical properties were examined at room temperature.

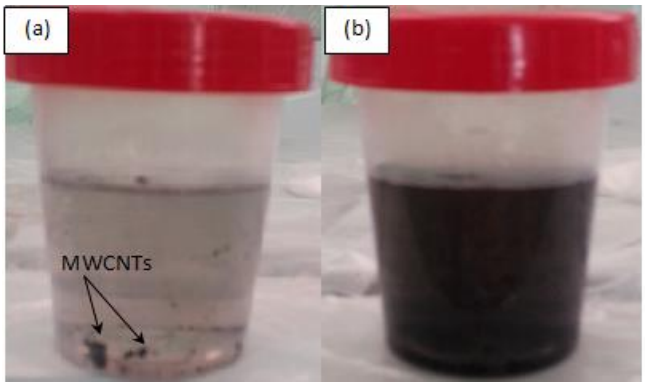

Fig. 1: exhibits MWCNTs suspension (a) before and (b) after sonication process.

Results and discussion

Fig.2 illustrates three dimension atomic force microscopy (AFM) and granularity accumulation distribution chart images for porous silicon prepared at 14mA/cm^2 for 17min which displays that the PSi consists of a matrix of arbitrary disseminated nanocrystalline Si pillars have the similar direction. The root mean square of surface roughness was 0.872nm, the porosity 68.67%, average grain size 50.9nm and roughness 0.736nm.

Fig.3 shows image of scanning electron microscopy (SEM) of n-PSi sample, with the assistance of the top view image of the sample, the black spots on the image were ascribed to the formation of the pores, where the white area representing the residual silicon (pore wall). The pores are spherical, asymmetrical in shape, and arbitrarily distributed on the porous matrix. The as-prepared layer has pores with various size and shapes. Further Jeyakumaran *et.al*.[8], found that the pore surface reveals an etched area having masses of nanocrystallites and these nanocrys-tallites too contended that it's possible that the intense photoluminescence (PL) at room temperature is occur because of the quantum confinement effect due to the aggregates existence in the PSi etched area . Fig.(4-a) demonstrates SEM image of multi wall carbon nanotubes pristine also the suspension dropped on a wafer of Si. It is exhibit an aggregation multi wall carbon nanotubes powder in the shape of approximately sphere-shaped and diameters ranged from few (nm-μm) because of the effect of agglomeration. While a side view of image of SEM of MWCNTs suspension dropped on Si wafer by drop casting after sonication reveals that the MWCNTs were separated to form independently tubes which its diameters ranging from (14.2 - 42.8)nm, was shown in fig.(4-b).

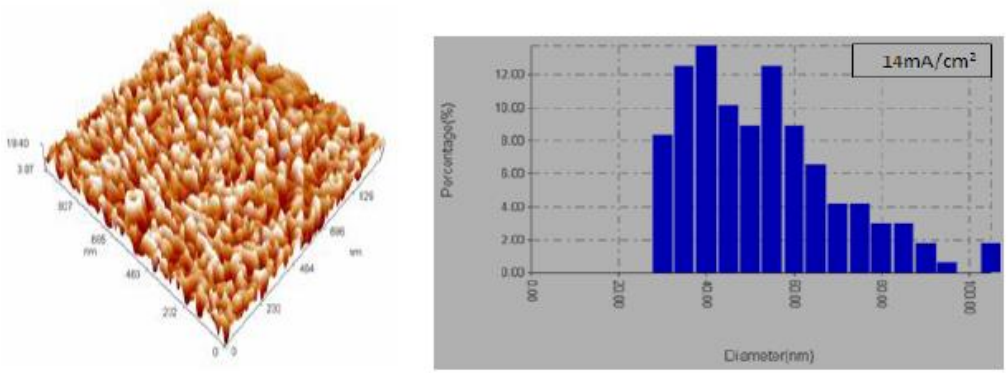

Fig. 2: 3D PSi surface AFM image and granularity accumulation distribution chart

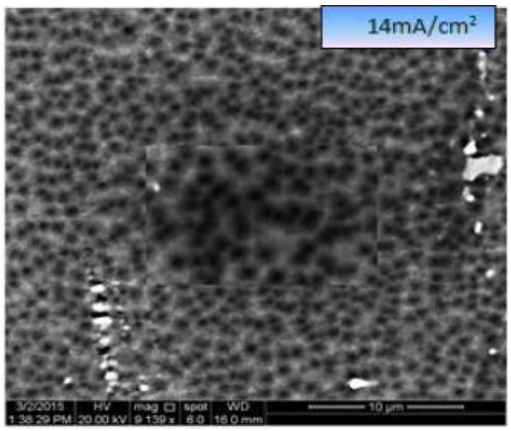

Fig. 3. Top view SEM of PSi

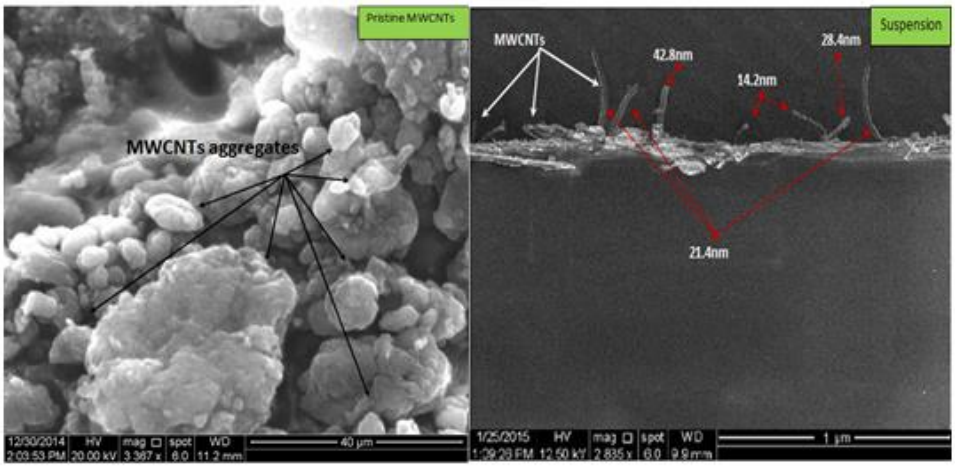

Fig. 4. SEM image of powder MWCNTs (left) and side view of MWCNTs layer dropped on silicon (right).

Fig.5 exhibits the microstructure of porous silicon by using the optical microscope. This micrograph showed that the porous silicon morphology enable simply recognized over the film homogeneousness and color. Fig.5 exhibits high density of tiny pores dispersed along the etched area. As well, the etched surface is rough and displayed different colors some time close to red resulting may be a sub oxide of silicon. There is no cracks or voids are noticed on layer surface.

Fig.6 shows XRD of crystalline silicon (n-type silicon) and PSi sample prepared at 14mA/cm^2 current density at 17min etching time. A peak of n-PSi illustrations a splitting peak located at (2θ = 33.7°) oriented only along the direction (211) (according to ICDD N 1997 and 2011 JCPDS). The n-PSi intensity peak was reduced. This result was attributed to ray diffraction from crystals with nanosize on the walls between pores. According to this figure, we can confirm that the PSi layer remains crystalline of the (211) peak. Further, the presence of this peak after etching process confirms that the cubic structure of the c-Si is reserved even after the formation of the pores and these results agree with[9][10][11]. This result is ascribed to effect of strain which leads to a little expanded lattice parameter as shown in Table (1).

The FTIR spectra of PSi are shown in fig.7. A chemical bonds and their IR resonance positions noticed in PSi are displayed in Table (2). These peaks positions are compared with others reported work and have found good matching[8][12][13] [14] [15].

Fig.8 exhibits the Fourier transformation infrared spectroscopy spectra of suspension MWCNTs ranging from (500-4000)cm$^{-1.}$ Peaks located in 932 and 2936cm^{-1} represent C-H symmetrical mode[3][16]. Misra *et. al.* recognized the peak at 1490 cm^{-1} as unparalleled to MWCNTs[17]. Also, bonds at 1582cm^{-1} can be refers to the structure of graphite in MWNTs[16]. C=C stretching vibration bond seems at 1668.43cm^{-1}[18] . A broad peak of transmission at 3444.87 cm^{-1} corresponds to (O-H) group, this result indicates a positive overview of the OH group on the side walls of the MWCNTs which inspire them certainly and easily spread in polar solvents like ethanol, water, DMF,… [19]. The peak at 1100cm^{-1} corresponding to the C-O stretch vibration mode[20].Fig.(9,a-b) clarifies the photoluminescence spectra (PL) of the PSi before and after depositing MWCNTs, respectively. Figure(9-a) exhibits an emission peak of PSi centered at 749nm and corresponded to 1.65 eV energy gap, while figure(9-b) shows the spectra of PL of MWCNTs deposited on n-PSi which shown a wide peak centered at 693 nm matched to1.78 eV. The depositing multi wall carbon nanotubes on n-PSi resulted in a beneficial 56nm blue shift, so that this can improve the wavelength detection of photovoltaic detectors of PSi, this result agree with[21]. The increasing of PL intensity of n-PSi was observed after depositing MWCNTs and this attributed to the reduced structural defects density in PSi.

Fig.10 shows the current-voltage forward and reverse in directions of dark characteristics of a PSi/Si photovoltaic detector before and after MWCNTs depositing process. The forward current increased after depositing MWCNTs and this occur because of reduced resistivity of porous layer which subsequently enhanced the On/Off ratio from (153.5-604). The ideality factor decreased from 3.9 to 3.21 and this occur because MWCNTs improved PSi/c-Si photodetector properties and the photodetector approach to an ideal diode.

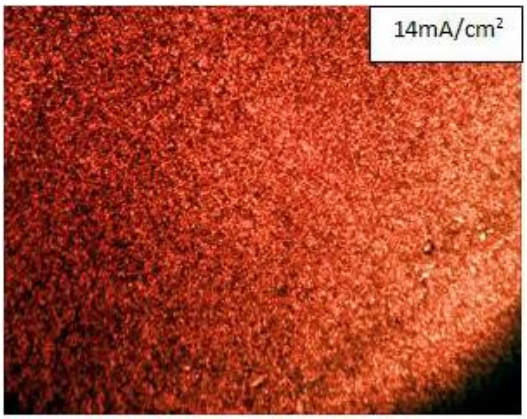

Fig. 5. Optical micrographs of porous silicon sample for 17min etching time, (M=1000X).

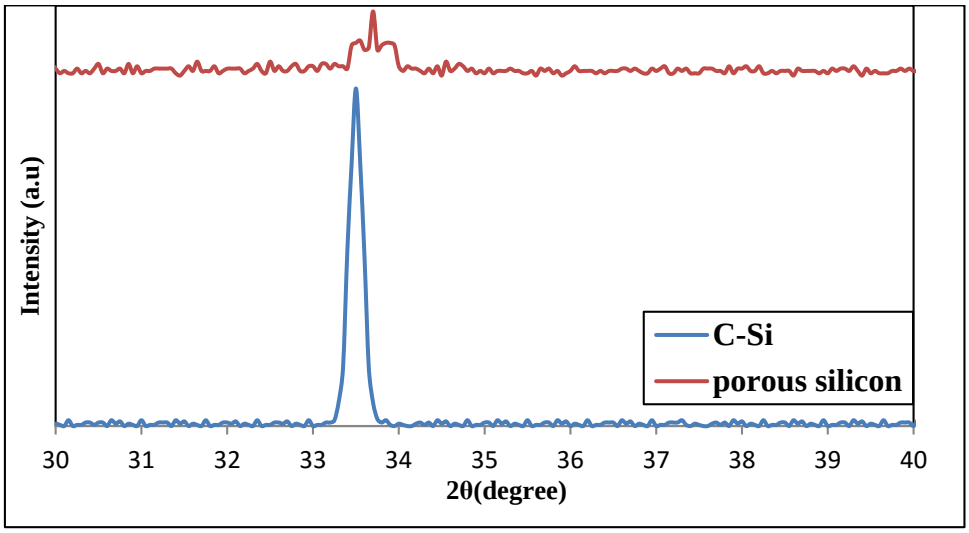

Fig. 6. XRD spectra of n-Si and porous silicon sample etched at 14mA/cm2 anodization current density for 17 min etching time.

Table 1: Calculated crystalline size, dislocation density and microstrain for porous silicon sample.

Anodization current density (mA/cm^2)	Anodization time (min)	2θ (deg)	FWHM (deg)	Crystallite size (nm)	Dislocation density $*10^{14}$ $(line.m)^{-2}$	Microstrain $*10^{-3}$ $lines^{-2}m^{-4}$
14	17	33.7	0.171	50.7	3.88	7.14

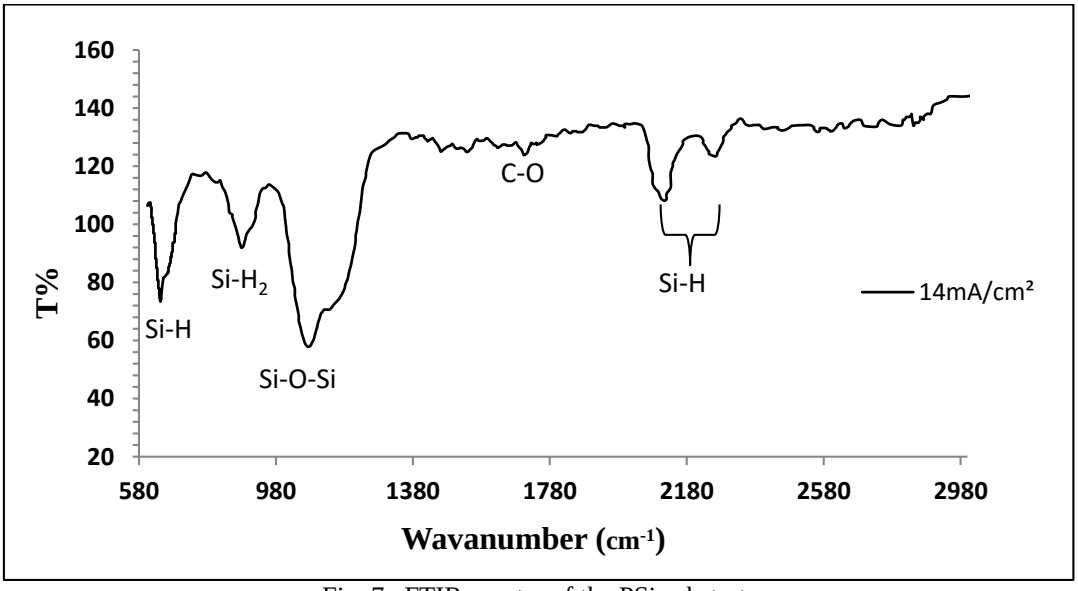

Fig. 7. FTIR spectra of the PSi substrate

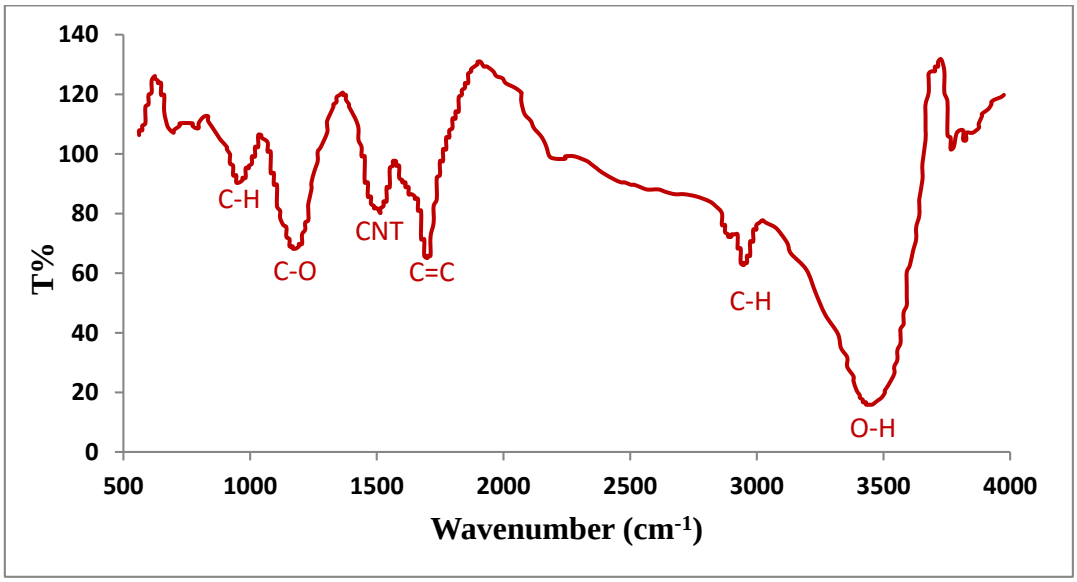

Fig. 8. FT-IR spectra of suspension MWCNTs.

Table 2: The Functional group and their Vibration mode in porous silicon

Functional group	Frequency	Bonds	
Si- H	638.46, 2260.65, 2088.98	Si3-SiH	Bending modes
SiH2	871.82	Si-H2	Wagging modes
Si-O-Si	1071	Si-O-Si	Asymmetry stretch
C-O	1683.91	C-O	Carbon Oxygen bond

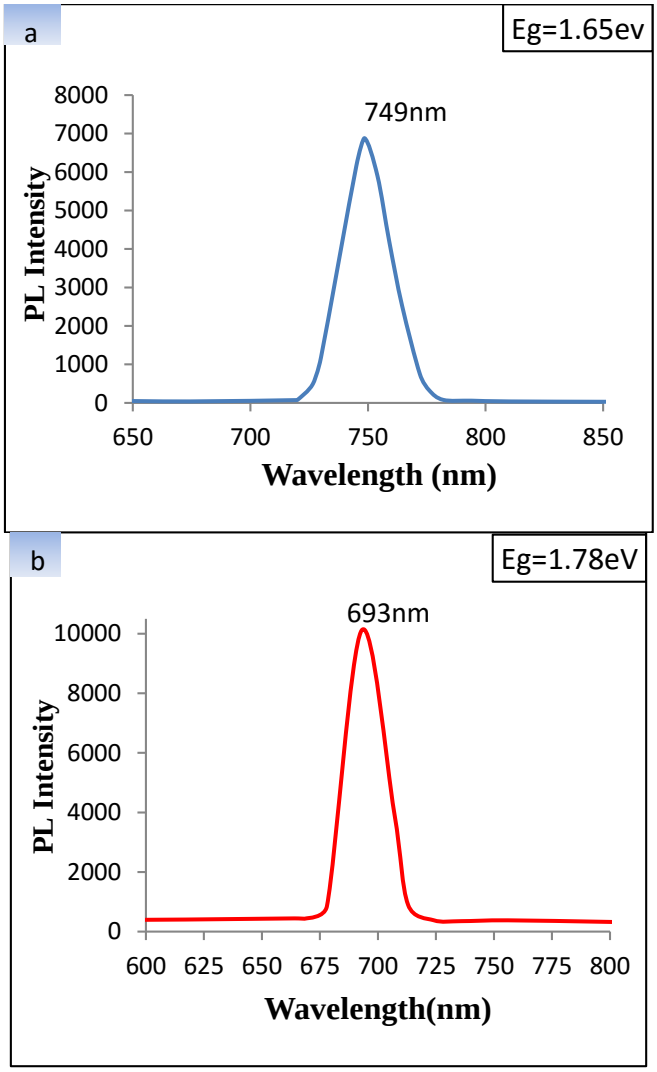

Fig. 9. PL spectra for (a) porous silicon and (b)MWCNTs/PSi/Si.

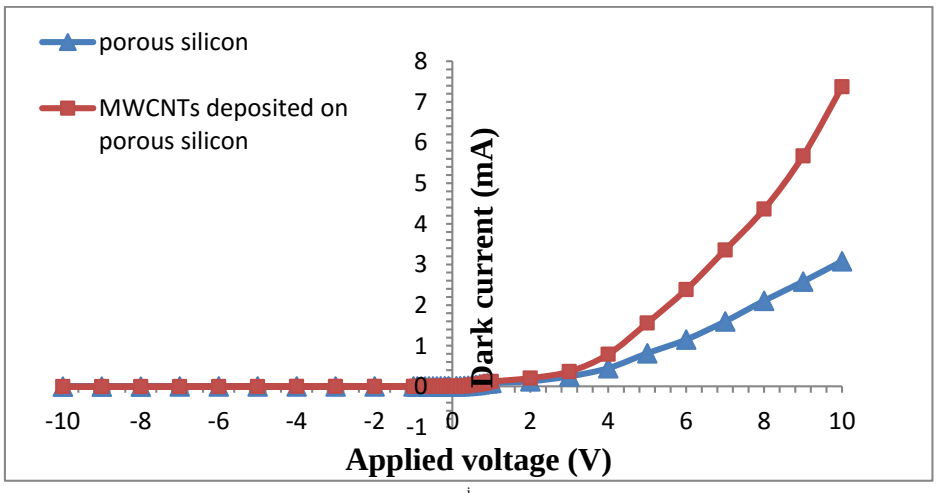

Fig. 10. Dark I–V characteristic of PSi/Si and MWCNTs/PSi/Si.

Fig. 11 shows the capacitance square reciprocal versus bias voltage of n-PSi/Si and MWCNTs/PSi/Si photovoltaic detectors. The V_{bi} was assessed by extrapolating the voltage axis linear part, V_{bi} decreased from 1.6 V to 1.2 V after depositing and this occur due to the increased porous layer conductivity. The junction was abrupt type and this observed from linear relationship.

Fig. (12-a) shows the spectral responsivity curve of n-PSi/Si and MWCNTs/PSi/Si photovoltaic detectors at reverse bias (5V). there are two response peaks were displayed; the first one at 650nm is created by the structure absorption edge of PSi, where as the other one at 900 nm refer to crystalline Si absorption edge. The increasing spectral responsivity after depositing CNTs can be attributed to the short diffusion length of photogenerated carriers and large surface area after depositing process[22]. The PSi obtained values of spectral responsivity were greater than that the values in articles [23][24][25]. The small shift in the response peak of photovoltaic detectors were noticed after depositing process, while fig.(12-b) shows the relationship of specific detectivity-wavelength for MWCNTs/PSi/n-Si photovoltaic detectors. It's obviously show an improved in specific detectivity after depositing and this occur due to reduction (I_n) noise current and increasing of spectral responsivity. Also, the maximum specific detectivity was found to be 4.1 × 1013W^{-1}cm $Hz^{1/2}$ at the wavelength 650 nm for MWCNTs/PSi/n-Si photodetector.

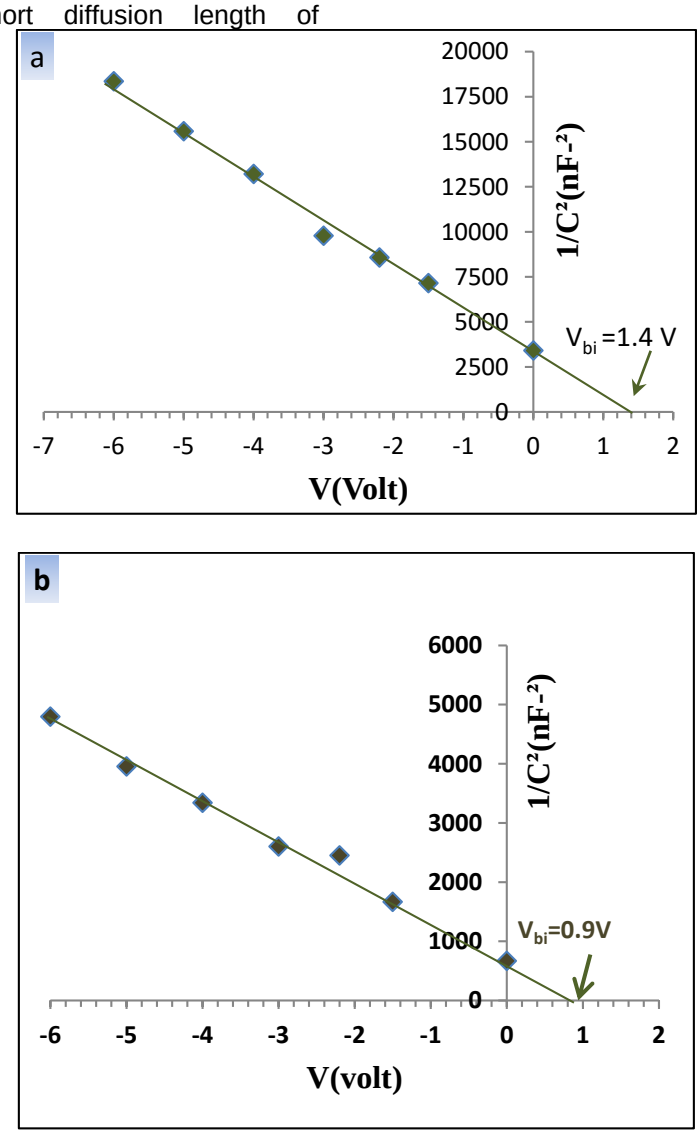

Fig. 11. $1/C^2$ as opposed to reverse bias voltage of PSi(a) before and (b) after depositing MWCNTs.

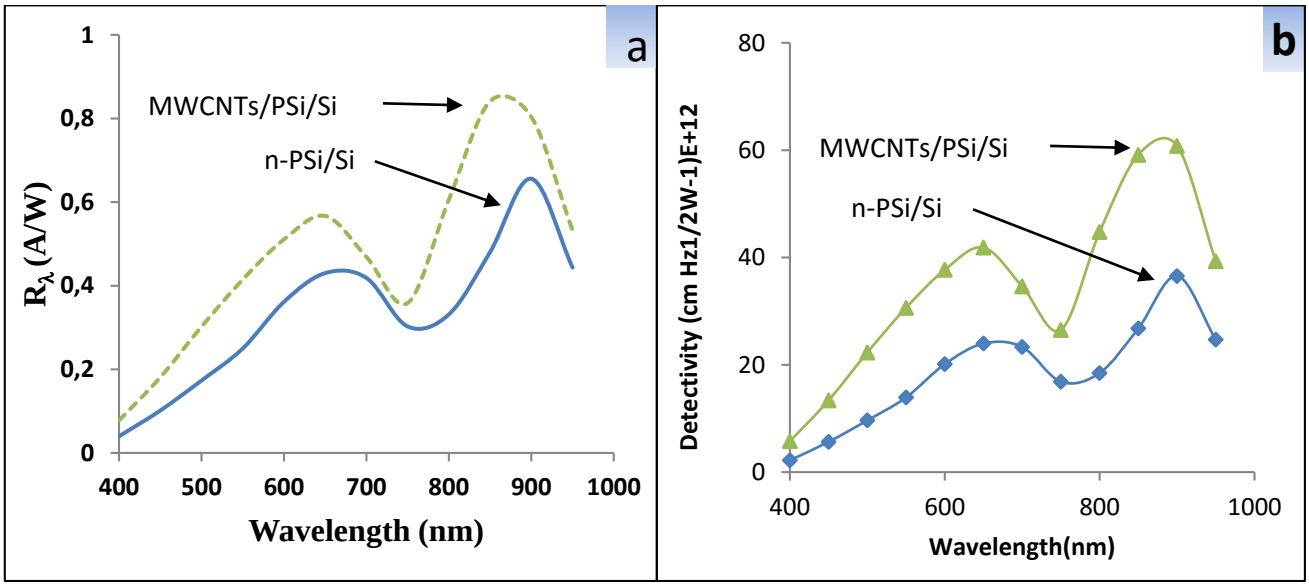

Fig.12. (a)Photosensitivity plot (b)specific detectivity for n-PSi/Si and MWCNTs-/PSi/Si photovoltaic detectors

Conclusion

Performance enhancement of PSi/n-Si photodetector by depositing the MWCNTs was presented. Photodetector photosensitivity was increased, ideality factor decreased, the tiny peak shift of response was observed this mean that the MWCNTs improved the electrical properties of Psi/n-Si photodetector after depositing process. There is no significant characteristics change in the photovoltaic detectors were gotten after

storing in laboratory environment. Finally, the designed multi wall carbon nanotubes (MWCNTs) based photodetector (MWCNTs/PSi/n-Si) has low cost, high sensitivity and reasonable speed for the UV-Vis spectral range without cooling.

References

[1] A. Salis, S. Setzu, M. Monduzzi, G. Mula, S. Chimiche, C. Csgi, D. Fisica, and U. Cagliari, "Porous Silicon-based Electrochemical Biosensors," *Elsevier*, 2010.

[2] N. Naderi and M.R. Hashim, "Effect of surface morphology on electrical properties of electrochemically-etched porous silicon photodetectors," *Int. J.Electrochem. Sci.*, vol. 7, pp. 11512–11518., 2012.

[3] F. Ronkel and J.W. Schultze, "Electrochemical Aspects of Porous Silicon Formation," *J. Porous Mater.*, vol. 7, pp. 11–16, 2000.

[4] W. Krätschmer, "Solid C60: a new form of carbon"," *Nature*, vol. 347, pp. 354 – 358, 1990.

[5] M. Kanungo, H. Lu, G.G. Malliaras, G.B. Blanchet, M. Kanungo, H. Lu, G.G. Malliaras and G.B. Blanchet, "Suppression of metallic conductivity of single-walled carbon nanotubes by cycloaddition reactions," *Science (80-.).*, vol. 80, pp. 234–237, 2009.

[6] E.S. Snow, P.M. Campbell, M.G. Ancona, J.P. Novak, "High-mobility carbon-nanotube thin-film transistors on a polymeric substrate," *Appl. Phys. Lett*, vol. 3, pp. 1–3, 2005.

[7] J. Appenzeller, "Carbon nanotubes for high-performance electronics—progress and prospect," *Proc. IEEE*, vol. 96, pp. 201–204, 2008.

[8] N. Jeyakumaran, B. Natarajan, S. Ramamurthy and V. Vasu, "Structural and optical properties of n- type porous silicon– effect of etching time," *Int. J. Nanosci. Nanotechnol.*, vol. 3, no. 1, 2008.

[9] U. M. Nayef and A. H. Jaafar, "Characteristics of Nanostructure Porous Silicon Prepared by Anodization Technique," *Eng. Tech. J.*, vol. 31, no. 3, pp. 339–347, 2013.

[10] U. M. Nayef, "Fabrication and Characteristics of Porous Silicon for Photoconversion," vol. 13, no. 02, pp. 61–65, 2013.

[11] Hassan Hadi, Raid Ismail and Nadir Habubi, "Fabrication and characterization of porous silicon layer prepared by photo-electrochemical etching in CH 3 OH : HF solution," *Int. Lett. Chem. Phys. Astron.*, vol. 3, pp. 29–36, 2013.

[12] Y. Al-Douri, N. M. Ahmed, N. Bouarissa and A. Bouhemadou, "Investigated Optical and Elastic Properties of Porous Silicon:Theoretical Study," *Mater. Des.*, vol. 32, pp. 4088–4093, 2011.

[13] B. K. Mohamid, U. M. Nayef, and Z. F. Kadem, "Chemical , Morphological and Electrical Properties of Porous Silicon Prepared by Photelectrochemical Etching," vol. 16, no. 4, pp. 145–151, 2013.

[14] I. M. Mohammed andA. H. Shnieshil, "Characteristics Study of Porous Silicon Produced by Electrochemical Etching technique," *Int. J. Appl. or Innov. Eng. Manag.*, vol. 2, no. 9, pp. 77–80, 2013.

[15] Z. Mengistu, L. DeSouza and S. Morin, "Functionalized porous silicon surfaces as MALDI-MS substrates for protein identification studies," *R. Soc. Chem.*, 2005.

[16] B. de Smet, H. Zuilhof, E. Sudhölter , G. Wittstock, M. Duerdin, L. Lie and A. Houlton, "Diffusion in porous silicon: effects on the reactivity of alkenes and electrochemistry of alkylated porous silicon," *Electrochim. Acta*, vol. 47, pp. 2653–2663, 2002.

[17] D. C. T. and M. R. M. J. M. P. K.R. Murali, "Synthesis of Porous Silicon Nanostructres for Photoluminescent Devices," *Mater Phys. Mech.*, vol. 4, pp. 143–147, 2001.

[18] N. Koshida, "Device Applications of Silicon Nanocrystals and Nanostructures.," *Tokyo, Japan: Springer,* 2009.

[19] P. Kumar, "Effect of Silicon Crystal Size on Photoluminescence Appearance in Porous Silicon," *Int. Sch. Res. Netw. ISRN Nanotechnol.*, vol. 1, pp. 1–6, 2011.

[20] H. T. Jung, D.H., Ko, Y.K., Jung, "Aggregation behavior of chemically attached poly(ethy-lene glycol) to single-walled carbon nanotubes (SWNTs) ropes," *Mater. Sci. Eng.c*, vol. 24, pp. 117–121, 2004.

[21] Raid A. Ismail, Raheem G. Kadhim and Wasna'a M. Abdulridha, "Effect of multiwalled carbon nanotubes incorporation on the performance of porous silicon photodetector," *Optik (Stuttg).*, vol. 127, pp. 8144–8152, 2016.

[22] P. Castrucci, C. Scilletta, S. Del Gobbo, M. Scarselli, L. Camilli, M. Simeoni, B. Delley, A. Continenza, M. De Crescenzi, "Light harvesting with multiwallcarbon nanotube/silicon heterojunctions," *Nanotechnology*, vol. 22, 2011.

[23] Raid A.Ismail, "Fabrication and Characterization of Photodetector Based on Porous Silicon," *Surf. Sci. Nanotech*, vol. 8, pp. 388–391, 2010.

[24] Khawla S. Khashan, Amany A. Awaad and Maysaa A.Mohamed, "Effect on Rapid Thermal Oxidation process on Electrical Properties of Porous Silicon," *Eng. Tech. J.*, vol. 27, no. 4, pp. 663–674, 2009.

[25] Husnen R. Abd, Y. Al-Douri, Naser M. Ahmed, U. Hashim and Raid A.Ismail, "Alternative-Current Electrochemical Etching of Uniform Porous Silicon for Photodetector Applications," *Int. J. Electrochem. Sci.*, vol. 8, pp. 11461 – 11473, 2013.